Journal of Statistical Physics, Vol. 43, Nos. 5/6, 1986

Path-Integral Monte Carlo Simulations of Electron Localization in Water Clusters

D. Thirumalai,[1] A. Wallqvist,[2] and B. J. Berne[2]

Path-integral Monte Carlo simulations are used to investigate the possibility of binding of an excess electron to water clusters. Model potentials are used to characterize the interaction between the excess electron and a water monomer and between two water molecules. The simulations reveal that two water molecules can bind an electron. In addition, it is found that the excess electron can be trapped in the field of three water molecules arranged in a linear configuration. The results are used to comment on recent molecular beam experiments.

INTRODUCTION

The Feynman path-integral approach[(1)] in Euclidean time is a powerful tool to simulate the equilibrium properties of many-body quantum systems.[(2)] In the last few years there have been numerous simulations of interacting quantum spin systems as well as those of many-body systems (for a brief review, see Ref. 3) interacting via well-known potentials at finite temperatures.[(4)] All of these examples exploit the path-integral formalism and the Trotter formula for the exponential of a quantum operator. In this paper a brief review of the use of the path-integral Monte Carlo technique to simulate the equilibrium properties of quantum systems at finite temperature, interacting with each other by specified pair potentials, is presented. We use this basic formulation to investigate the localization of an excess electron by clusters comprised of finite number of water molecules.[(5)] This is an important problem because an understanding of the nature of

[1] Department of Chemistry and Biochemistry and Institute for Physical Science and Technology, University of Maryland, College Park, Maryland 20742.
[2] Department of Chemistry, Columbia University, New York, N.Y. 10027.

0022-4715/86/0600-0973$05.00/0

electron states in these systems can be used to describe the general phenomena of an excess electron in polar liquids.[6] Many of the models that have been used to predict the structural and dynamical properties of an electron in polar solvents have been purely phenomenological in nature. We were motivated to explore the behavior of an excess electron in water clusters not only because of its obvious importance in a variety of physical situations but also by the recent molecular beam experiments by Haberland et al.[7,8] They have examined the stability of e^-–$(H_2O)_n$ systems as a function of n, the number of water molecules comprising a cluster, in molecular beam experiments. They showed that the e^-–$(H_2O)_n$ is stable when $n \geqslant 11$. More surprisingly, it is claimed that, when the beam of water molecules is seeded with Ar atoms to effectively lower the beam temperature, two water molecules can localize an electron. They also assert that e^-–$(H_2O)_n$ is not stable for $n = 3$, 4, or 5. Spurred by these findings we began to explore the stability and structure of an electron interacting with water clusters. Our calculations are based on model potentials. Path-integral Monte Carlo methods are then used to investigate the possibility of electron localization in water clusters as a function of the cluster size. This method is probably not as accurate as ab initio calculations but is applicable to larger clusters. In particular, it is hoped that by obtaining model potentials that describe the energetics of electron–water clusters fairly accurately one can use them in quantum mechanical simulations of an electron in liquid water.[9,11] (For a related review, see Ref. 10). In this article we discuss our results for the stability and structure of e^-–$(H_2O)_n$ system for $n = 2$ and 3 using path-integral Monte Carlo (PIMC) techniques.

This review is organized as follows. In Section 2 we discuss the methodology of PIMC as it applies to electron localization in water clusters. Section 3 describes the calculations and the results. We conclude with a discussion in Section 4.

THEORY

In this section we discuss the implementation of the path-integral Monte Carlo method and the particular way it is exploited for the problem considered here. The formulation presented here is applicable to any N-body problem. The Hamiltonian of the excess electron interacting with N water molecules can be written as

$$H = \frac{\vec{p}^2}{2m} + \sum_{i=1}^{N} \sum_{\alpha=1}^{3} \frac{\vec{P}_{i(\alpha)}^2}{2M_\alpha} + \sum_{i<j} V(\vec{R}_i, \vec{R}_j) + \sum_{i=1}^{N} U(\vec{r}, \vec{R}_i) \tag{1}$$

$$\equiv T + V_T$$

where $\vec{r}$, $\vec{p}$ denote the coordinate of the electron and the momentum conjugate to $\vec{r}$, $\vec{P}_{i(\alpha)}$ is the momentum of the αth species of the ith water molecule and M_α is the corresponding mass, where $M_1 = M_O$ and $M_{2,3} = M_H$ are the oxygen and hydrogen masses respectively, $\vec{R}_i$ denotes the collection of the coordinates of the ith water molecules, $V(\vec{R}_i, \vec{R}_j)$ is the potential of interaction between water molecules, and $U(\vec{r}, \vec{R}_i)$ is the interaction potential between the excess electron and the ith water molecule. The quantity of interest is the canonical partition function Q for the Hamiltonian at the temperature T which is given by

$$Q = \mathrm{tr}(e^{-\beta H/P})^P \tag{2}$$

If we neglect the exchange contribution[3] due to the indistinguishability of the water molecules we can insert unity in the form

$$\int d\vec{R}\, d\vec{r}\, |\vec{R}, \vec{r}\rangle\langle\vec{R}, \vec{r}|$$

with $|\vec{R}, \vec{r}\rangle = |\vec{R}_1, \vec{R}_2, \ldots, \vec{R}_N, \vec{r}\rangle$, P times in (2) to write Q in this representation as

$$Q = \prod_{t=1}^{P} \int d\vec{R}^{(t)}\, d\vec{r}^{(t)} \langle \vec{R}^{(t)}, \vec{r}^{(t)} | e^{-\varepsilon H} | \vec{R}^{(t+1)}, \vec{r}^{(t+1)} \rangle \tag{3}$$

In (3) $\varepsilon = \beta/P$ and $\vec{R}^{(P+1)} = \vec{R}^{(1)}$, and $\vec{r}^{(P+1)} = \vec{r}^{(1)}$. If ε is small, which can be arranged by making P sufficiently large, then we can use the Trotter formula

$$e^{-\varepsilon(T+V_T)} = e^{(-\varepsilon/2)V_T} \cdot e^{-\varepsilon T} \cdot e^{(-\varepsilon/2)V_T} + O(\varepsilon^2) \tag{4}$$

where the Hamiltonian is split into a kinetic energy term and a potential energy piece with

$$T = \frac{\vec{p}^2}{2m} + \sum_{i=1}^{N} \sum_{\alpha=1}^{3} \frac{\vec{P}_{i(\alpha)}^2}{2M_\alpha} \tag{5}$$

In the coordinate representation (4) becomes

$$\begin{aligned} &\langle \vec{R}^{(t)}, \vec{r}^{(t)} | e^{-\varepsilon H} | \vec{R}^{(t+1)}, \vec{r}^{(t+1)} \rangle \\ &\quad = \left(\frac{mP}{2\pi\hbar^2\beta}\right)^{3/2} \left(\frac{M_O P}{2\pi\hbar^2\beta}\right)^{3N/2} \left(\frac{M_H P}{2\pi\hbar^2\beta}\right)^{3N} \exp\left\{ -\left[\frac{\varepsilon}{2} V_T(\vec{R}^{(t)}, \vec{r}^{(t)}) \right.\right. \\ &\qquad + \sum_{i=1}^{N} \sum_{\alpha=1}^{3} \frac{M_\alpha (\vec{R}_{i(\alpha)}^{(t)} - \vec{R}_{i(\alpha)}^{(t+1)})^2}{2\hbar^2\varepsilon} + \frac{m}{2\hbar^2\varepsilon} (\vec{r}^{(t)} - \vec{r}^{(t+1)})^2 \\ &\qquad \left.\left. + \frac{\varepsilon}{2} V_T(\vec{R}^{(t+1)}, \vec{r}^{(t+1)}) \right] \right\} \end{aligned} \tag{6}$$

[3] The mean distance between the atoms is so large that the major contribution to the partition function comes from the direct paths.

Substituting (6) into (2) the partition function in the discretized path-integral formulation can be written as

$$Q_p = \left(\frac{mP}{2\pi\hbar^2\beta}\right)^{3P/2} \left(\frac{M_O P}{2\pi\hbar^2\beta}\right)^{3NP/2} \left(\frac{M_H P}{2\pi\hbar^2\beta}\right)^{3NP} \times \int \exp(-S_{\text{eff}}) \prod_{i=1}^{N} \prod_{j=1}^{P} d\vec{R}_i^{(j)}\, d\vec{r}^{(j)} \tag{7}$$

$$S_{\text{eff}} = \beta(V_{e-W} + V_{W-W}) \tag{8a}$$

$$V_{e-W} = \sum_{j=1}^{P} \left[\frac{mP}{2\hbar^2\beta^2}(\vec{r}^{(j)} - \vec{r}^{(j+1)})^2 + \frac{1}{P}\sum_{i=1}^{N} V(\vec{r}^{(j)}, \vec{R}_i^{(j)})\right] \tag{8b}$$

and

$$V_{W-W} = \sum_{i=1}^{N} \left\{ \sum_{j=1}^{P} \left[\sum_{\alpha=1}^{3} \frac{M_\alpha P}{2\hbar^2\beta^2} (\vec{R}_{i(\alpha)}^{(j)} - \vec{R}_{i(\alpha)}^{(j+1)})^2 + \frac{1}{2P} \sum_{k\neq i}^{N} V(\vec{R}_i^{(j)}, \vec{R}_k^{(j)}) \right] \right\} \tag{8c}$$

Thus in the discretized path-integral formulation the system consisting of $3N+1$ quantum particles is isomorphic to $3NP+P$ classical particles moving in a potential field given by (8). This formulation allows us to evaluate Q and all the relevant properties (like energy and distribution functions) by classical Monte Carlo techniques. If the isomorphic classical system is ergodic, then one can also use molecular dynamics to evaluate the equilibrium properties.[12] The conditions under which one expects the molecular dynamics method for quantum mechanical systems to be unreliable is given elsewhere.[13] It should be pointed out that there are ways to circumvent these difficulties.[14,15] For the problem of the binding of an electron to water clusters we have chosen to use the Metropolis Monte Carlo method[16] to calculate the properties of interest.

RESULTS AND DISCUSSION

The calculations are performed by equilibrating the isomorphic classical system consisting of $3NP+P$ particles moving in an effective potential given by (8). The initial configuration of the isomorphic system is arbitrary, and the results reported here are independent of the starting configuration. The stability of the e^-–$(H_2O)_n$ is determined by (a) the overall external potential energy between the electron and water clusters, (b) the behavior of the external electron–oxygen radial distribution function $g_{eO}(r)$, and (c) examination of the configurations of the e–$(H_2O)_n$ system.

The nature of the electron state is inferred from $g_{eO}(r)$ and by inspecting the configurations generated during the simulation. Unless otherwise stated all the calculations were done at 5K. Before presenting the results we briefly describe the interaction potentials $V(\vec{R}_i, \vec{R}_j)$ and $U(\vec{r}, \vec{R}_i)$. The term $V(\vec{R}_i, \vec{R}_j)$ is taken to be the modified central force potential of water. The internal vibrations of the water molecule are modeled by a set of Morse potentials.[17] The electron–water monomer interaction $U^{\mathrm{I}}(\vec{r}, \vec{R}_i)$ consists of three terms: (a) an exponential repulsive interaction due to the closed shell electrons; (b) an anisotropic electron–dipole interaction centered in the center of charge of the water molecule and (c) an electron-induced dipole interaction due to the water polarizability centered on the oxygen atom. In order to assess the role of the polarizability of the water molecules (term c) another model potential, to be referred to as $U^{\mathrm{II}}(\vec{r}, \vec{R}_i)$, was constructed by omitting the third term in $U^{\mathrm{I}}(\vec{r}, \vec{R}_i)$. The details of these potentials are given elsewhere.[5]

The results reported here were obtained by averaging over 13,000 passes[5] after the system equilibrated. In all calculations the number of pseudoparticles for the electron was taken to be 1,000, and the number of

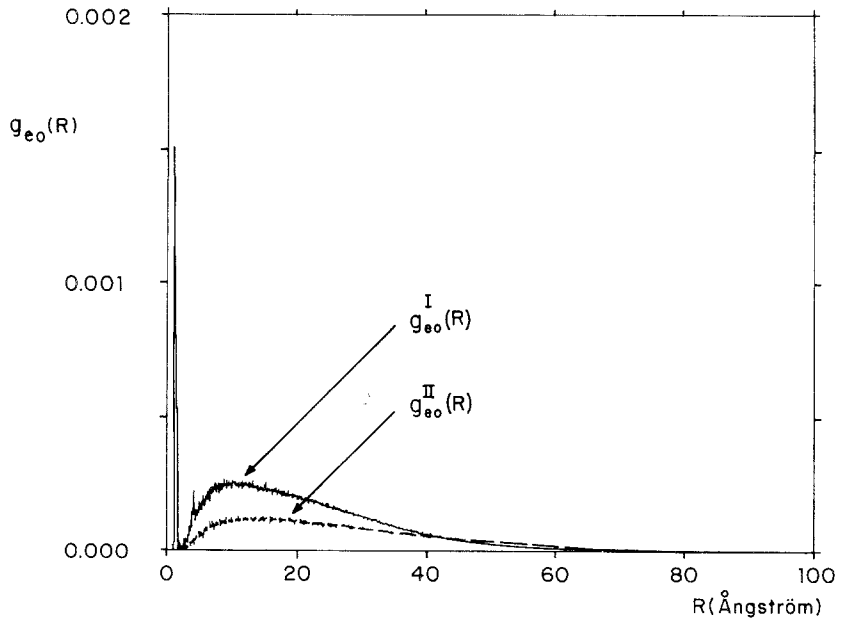

Fig. 1. Plot of the electron–oxygen radial distribution functions $g^{\mathrm{I}}_{eO}(r)$ and $g^{\mathrm{II}}_{eO}(r)$ as a function of r calculated using $U^{\mathrm{I}}(\vec{r}, \vec{R}_i)$ and $U^{\mathrm{II}}(\vec{r}, \vec{R}_i)$, respectively, for the electron–water dimer system.

pseudo particles in the hydrogen and oxygen chains was set to 100. In Fig. 1 a plot of the electron–oxygen radial distribution function $g_{eO}(r)$ given by

$$g_{eO}(r) = \left\langle \frac{1}{NP} \sum_{i=1}^{N} \sum_{t=1}^{P} \delta(|\vec{r}^{(t)} - \vec{R}_{iO}^{(t)}| - r) \right\rangle \tag{9}$$

as a function of r is presented. The two curves labeled $g_{eO}^{I}(r)$ and $g_{eO}^{II}(r)$ were calculated using $U^{I}(\vec{r}, \vec{R}_i)$ and $U^{II}(\vec{r}, \vec{R}_i)$, respectively. The solid line

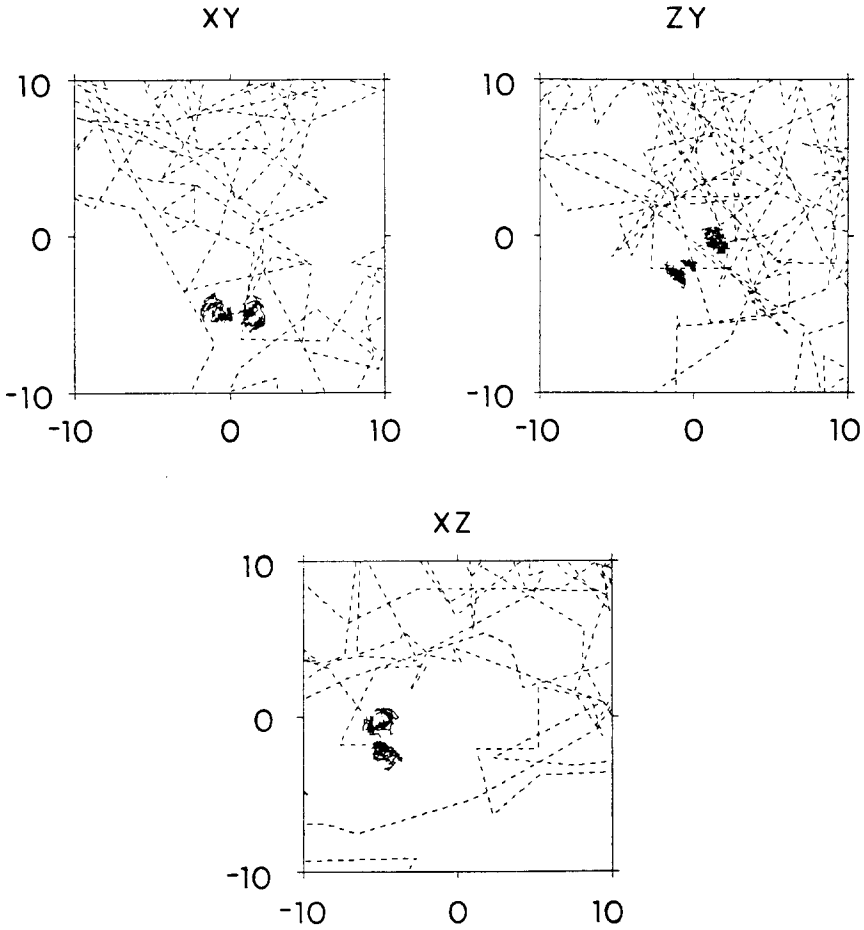

Fig. 2. This figure shows the instantaneous projection of the coordinates of the bound electron–water dimer system onto the xy, zy, xz planes. The coordinates of the isomorphic electron polymer chain are connected by dotted lines. The coordinates of the water molecules are connected by dark lines. The electron polymer chain is highly diffuse whereas the water molecules are very localized.

representing $g^{I}_{eO}(r)$ shows a peak in the electron density for $r > 2$ Å followed by a slowly decaying tail with a range of about 30–40 Å. A qualitatively similar result is indicated by $g^{II}_{eO}(r)$. However, the peak at $r \sim 9$ Å is much less pronounced, but the range remains the same. These curves clearly indicate that the bound electron can be characterized as being in a diffuse state. It is clear that the inclusion of the polarizability of the water molecule seems to increase the strength of the binding of the electron to the water dimer. This is reflected in the binding energy, which is found to be about 3–6 meV using $U^{I}(\vec{r}, \vec{R})$, whereas it is lowered to about 2–3 meV using $U^{II}(\vec{r}, \vec{R})$.

In order to gain insight into the geometry of the electron-dimer system we present a portion of the coordinates of the isomorphic classical system projected onto the xy, zy, and xz planes in Fig. 2. This figure shows that the electron is in a diffuse orbital, and inspection of the whole figure shows that the spatial extent of the electron cloud is as large as 100 Å. It is transparent from this figure that the two water molecules are located on the fringes of the electron cloud and that the electron density is anisotropically distributed around the water dimer.

We now turn our attention to the binding of an electron to a water trimer. The water trimer can exist in many different configurations which can be classified[18] according to the number of hydrogens of the central molecule that participate in hydrogen bonding. We confine ourselves to one such configuration labeled as the single donor linear conformer (SDC). In this configuration one of the hydrogens of the central molecule is engaged in hydrogen bonding, whereas the hydrogens of the two terminal molecules are free, resulting in an open linear configuration. As in the electron-water dimer case the e^{-}–$(H_2O)_3$ was equilibrated starting from various arbitrary initial configurations, and various quantities of interest were calculated by averaging over 13,000 passes after the initial equilibration. The results obtained were independent of the starting configurations. In Fig. 3 we plot the electron–oxygen radial distribution functions $g^{I}_{eO}(r)$ and $g^{II}_{eO}(r)$ using model potentials $U^{I}(\vec{r}, \vec{R}_i)$ and $U^{II}(\vec{r}, \vec{R}_i)$, respectively. It is clear that there is a substantial peak in $g^{I}_{eO}(r)$ at $r \sim 10$ Å, followed by a slowly decaying tail that eventually vanishes at $r \sim 40$ Å. The dashed line denoting $g^{II}_{eO}(r)$ also shows a peak at $r \sim 10$ Å, but the range is longer. There is a dramatic decrease in the peak height at $r \sim 10$ Å in $g^{II}_{eO}(r)$ as compared to the one in $g^{I}_{eO}(r)$. This is clearly an indication that the polarizability term plays a key role in enhancing the strength of the binding of the electron to the SDL trimer molecule. Both $g^{I}_{eO}(r)$ and $g^{II}_{eO}(r)$ exhibit a slowly decaying tail indicating that the electron is in a very diffuse surface state. It is interesting to compare $g_{eO}(r)$ to the electron-dimer and the electron-trimer systems and this is shown in Fig. 4. This figure shows that the

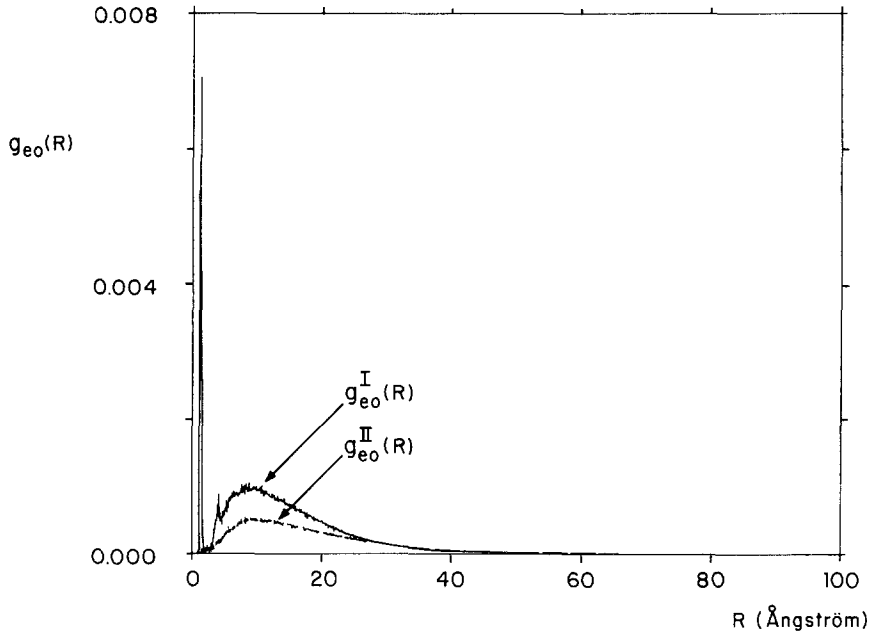

Fig. 3. Same as Fig. 1 except for the electron–water trimer system. The water trimer is in the single donor linear (SDL) configuration.

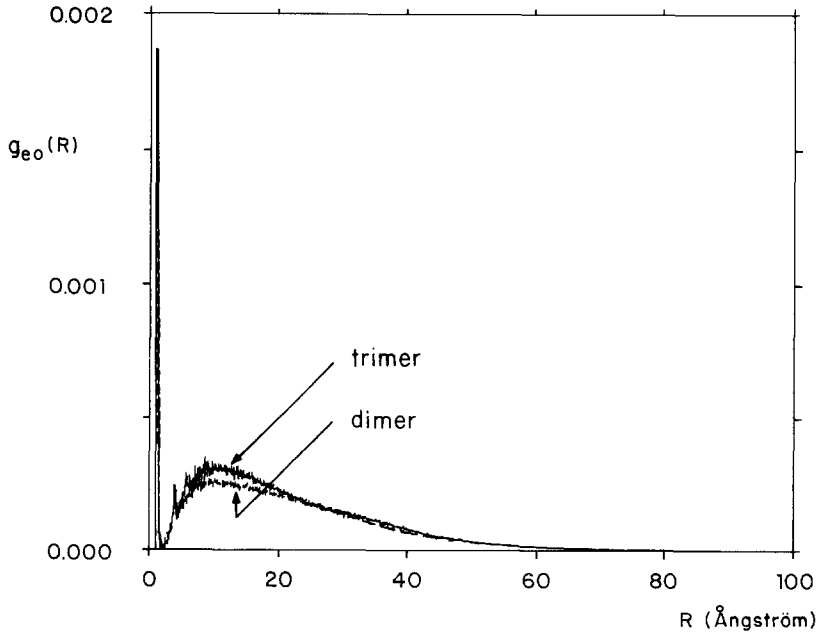

Fig. 4. Comparison of the electron–oxygen radial distribution functions between the e^-–$(H_2O)_3$ and the e^-–$(H_2O)_2$. Both curves were calculated using $U^I(\vec{r}, \vec{R}_i)$.

peak height at $r \sim 10$ Å is smaller for the e^-–$(H_2O)_2$ than it is for the e^-–$(H_2O)_3$. Both curves show a very sharp peak at $r < 2$ Å, which is a consequence of the trapping of the electron density by the deep well present in the electron-monomer potential.[5] In addition, there is a peak in $g_{eO}(r)$ corresponding to the electron–water trimer at $r \sim 5$ Å which is absent in the dimer radial distribution function. This peak corresponds to the presence of electron density near another water molecule and suggests that the electron is essentially localized by the field of two water molecules, with the third one playing a lesser role. The comparison in Fig. 4 also suggests that the excess electron is more strongly localized by the water trimer than by the

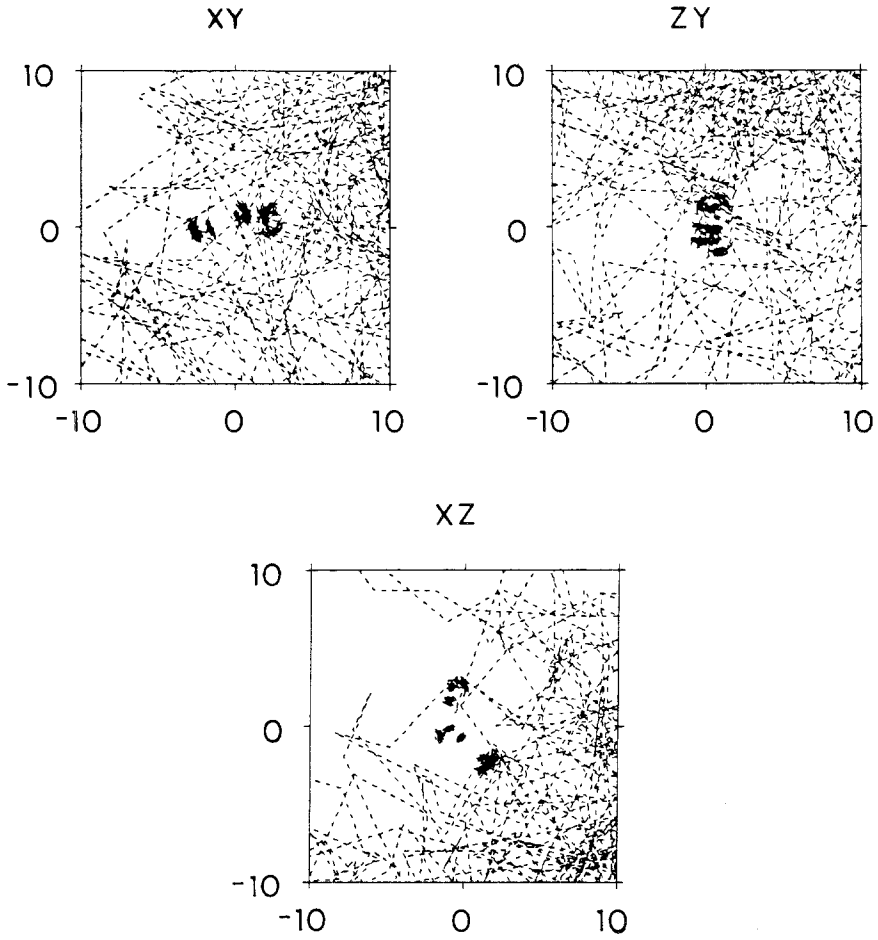

Fig. 5. Projections of the coordinates of the isomorphic electron–water trimer system onto the xy, zy, xz planes.

water dimer. This is consistent with the higher binding energy for the electron-trimer system (estimated to be between 4 and 9 meV) compared to the electron-dimer system.

Because the $g_{eO}(r)$ only represents an angularly averaged quantity it is of interest to look for other evidence of the electron density distribution. We have done this by projecting the coordinates of the isomorphic classical system onto the xy, zy, xz planes shown in Fig. 5. This demonstrates that the water molecules are confined to a small volume in space, whereas the electron is spatially extended. It clearly shows the anisotropy in the electron distribution and also allows one to unequivocally infer that the electron is in a diffuse surface state.

In light of these calculations what can one say about the stable electron-water dimer and the improbability of observing the stable electron-water trimer in the recent molecular beam experiments? To partially answer this question we examined the temperature dependence of the stability of the electron-water dimer system. The calculations were repeated at $T = 20$K and the results indicated that the excess electron does not bind to the water dimer. This is consistent with the low binding energy. Thus, unless the beam temperature is very low, these calculations do not explain the mechanism of the formation of the stable electron-water dimer in a molecular beam. The lack of prominence of the e^-–$(H_2O)_3$ peak seen in the recent molecular beam suggests that the predominant trimer conformer formed in a molecular beam is the one in which all three oxygen atoms are equivalent and where each water molecule has one hydrogen atom involved in hydrogen bonding. This conformer is called the single donor cyclic conformer (SDC). Our calculations[5] indicated that the excess electron is not localized by three water molecules in the SDC configuration. However, Haberland et al. note that when the beam was seeded with Xe instead of Ar they were able to detect weak signals corresponding to the e^-–$(H_2O)_3$ system. This suggests that Xe may facilitate the formation of the trimer in the SDL configuration. It would be desirable to perform further experiments to confirm our prediction that if SDL trimer conformer can be formed the resultant anion is more stable than the dimer anion.

CONCLUSIONS

In this paper, using path-integral Monte Carlo methods, we have explored the possibility of electron localization in water clusters. The major conclusions of our study are:

(a) It is shown that two water molecules can localize an electron. The excess electron is in a spatially diffuse surface state and the binding

energy of the electron-dimer at 5K is estimated to be between 3–6 meV. The attached electron does not induce major structural changes in the water dimer, which is consistent with the weak binding energy. These results are in accord with the LCAO–MO–SCF calculations of Chipman.[19]

(b) The inclusion of the spherical polarizability term enhances the strength of localization and gives rise to larger binding energy.

(c) A trimer molecule in the single donor linear conformer localizes the excess electron and the binding energy is estimated to be between 4–9 meV. As in the case of the electron-dimer system, the electron is in a diffuse surface state.

One of the major advantages of path-integral Monte Carlo calculations is the insight that one gets by examining the details of quantum many-body systems. In the example considered here it is practically impossible to experimentally determine the electron distribution or the structure of the water molecule around the electron. The hope is that these insights will enable us to construct appropriate models whose theoretical treatments will shed light on analogous complex systems. As was pointed out in the Introduction, quantum Monte Carlo simulations are finding increasing use in virtually all of physics where progress in analytical treatment is at present prohibitively difficult. In this spirit, quantum Monte Carlo is being used to study problems in fields ranging from particle physics[20] to biological sciences.[21] It is toward this end that quantum Monte Carlo simulations can be of great use.

ACKNOWLEDGMENTS

This work was supported in part by grants from the National Science Foundation and the National Institutes of Health. One of us (D. T.) wishes to acknowledge the partial support by the Camille and Henry Dreyfus foundation in the form of the distinguished new faculty award. D. T. also thanks T. R. Kirkpatrick for reading this manuscript.

REFERENCES

1. R. P. Feynman, *Rev. Mod. Phys.* **20**:367 (1948); R. P. Feynman and A. R. Hibbs, *Quantum Mechanics and Path Integrals* (McGraw Hill, New York, 1965).
2. H. F. Jordan and L. D. Fosdick, *Phys. Rev.* **171**:128 (1968); J. A. Barker, *J. Chem. Phys.* **70**:2914 (1979).
3. D. J. Scalapino, *Phys. Scrip.* **T9**:203 (1985).
4. For a review see D. Thirumalai and B. J. Berne, *Ann. Rev. Phys. Chem.* (to be published).
5. A. Wallqvist, D. Thirumalai, and B. J. Berne, *J. Chem. Phys.* (submitted for publication).

6. G. A. Kenney-Wallace, *Acc. Chem. Res.* **11**:433 (1978), and references therein.
7. H. Haberland, H. G. Schindler, and D. R. Worsnop, *Ber. Bunsenges. Chem.* **88**:270 (1984); *J. Phys. Chem.* **88**:3903 (1984).
8. H. Haberland, C. Lindewight, H. G. Schindler, and D. R. Worsnop, *J. Chem. Phys.* **81**:3742 (1984).
9. A. Wallqvist, D. Thirumalai, C. Pangali, and B. J. Berne (to be published).
10. P. J. Rossky, J. Schnitker, and R. A. Kuharski, *J. Stat. Phys.* **43**:949 (986).
11. For other simulations of an excess electron in polar solvents see M. Sprik, R. Impey, and M. L. Klein, preprint (NRCC, Canada, 1985); C. D. Jonah, C. Romero, and A. Rahman, *Chem. Phys. Lett.* **123**:209 (1986).
12. M. Parrinello and A. Rahman, *J. Chem. Phys.* **80**:860 (1984).
13. R. W. Hall and B. J. Berne, *J. Chem. Phys.* **81**:3641 (1984).
14. A. Wallqvist and B. J. Berne, *Chem. Phys. Lett.* **117**:214 (1985).
15. J. Kogut, Lecture at the Conference on Frontiers in Quantum Monte Carlo, Los Alamos, Sept. (1985).
16. N. Metropolis, A. W. Rosenbluth, M. N. Rosenbluth, A. H. Teller, and E. Teller, *J. Chem. Phys.* **21**:1087 (1953).
17. J. R. Reimers and R. O. Watts, *Chem. Phys. Lett.* **94**:222 (1982); *Chem. Phys.* **85**:83 (1984).
18. J. R. Reimers and R. O. Watts, *Mol. Phys.* **52**:357 (1984).
19. D. Chipman, *J. Phys. Chem.* **83**:1657 (1979).
20. For a review see J. Kogut, *Rev. Mod. Phys.* **55**:775 (1983).
21. A. Kuki and P. G. Wolynes (work in progress).